

Magnetic, conductive textile for multipurpose protective clothing and hybrid energy harvesting

Cite as: Appl. Phys. Lett. **118**, 143901 (2021); <https://doi.org/10.1063/5.0044022>

Submitted: 13 January 2021 . Accepted: 16 March 2021 . Published Online: 05 April 2021

 Ji Wan, Hang Guo, Haobin Wang, Liming Miao,  Yu Song, Chen Xu, Zehua Xiang, Mengdi Han, and  Haixia Zhang



View Online



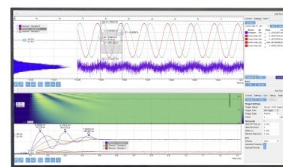
Export Citation



CrossMark

Challenge us.

What are your needs for periodic signal detection?



Zurich Instruments



Magnetic, conductive textile for multipurpose protective clothing and hybrid energy harvesting

Cite as: Appl. Phys. Lett. **118**, 143901 (2021); doi: [10.1063/5.0044022](https://doi.org/10.1063/5.0044022)

Submitted: 13 January 2021 · Accepted: 16 March 2021 ·

Published Online: 5 April 2021



View Online



Export Citation



CrossMark

Ji Wan,¹  Hang Guo,^{1,2} Haobin Wang,¹ Liming Miao,¹ Yu Song,¹  Chen Xu,^{1,2} Zehua Xiang,¹ Mengdi Han,^{3,a)} and Haixia Zhang^{1,2,a)} 

AFFILIATIONS

¹National Key Laboratory of Science and Technology on Micro/Nano Fabrication, Institute of Microelectronics, Peking University, Beijing 100871, China

²Academy for Advanced Interdisciplinary Studies, Peking University, Beijing 100871, China

³Department of Biomedical Engineering, College of Future Technology, Peking University, Beijing 100871, China

^{a)}Authors to whom correspondence should be addressed: hmd@pku.edu.cn and hxzhang@pku.edu.cn

ABSTRACT

In this paper, we report a magnetic and conductive textile made from a mixture of NdFeB microparticles, multi-walled carbon nanotubes, and polydimethylsiloxane. The textile can (i) shield 99.8% of electromagnetic signals ranging from 30 MHz to 3 GHz, thereby protecting people from damage caused by the electromagnetic radiation, (ii) be hydrophobic and fire retardant, making it a possible choice for raincoat and fire protection clothing, and (iii) convert mechanical energy into electricity through both electromagnetic induction and triboelectrification. The textile creates many opportunities in the fields of multifunctional protective equipment and energy harvesting.

Published under license by AIP Publishing. <https://doi.org/10.1063/5.0044022>

Integrating functional devices with traditional clothes and directly designing multifunctional smart clothes represent two attractive strategies that leverage the advancements of wearable technology to improve human health. The study of textile is of great importance, as textile is the key material to fabricate clothes. Improving the properties of textile or introducing new capabilities to textile can yield advanced clothes with many appealing features.^{1–3} Currently, many researchers are also focusing on improving the performance of the textile to ensure that people with better protection meet the requirement of specific applications, including electromagnetic shielding,^{4–6} flame retardancy,^{7,8} and many others. Nevertheless, few works report the design of textiles that can provide protection in different scenarios, due to the tough requirements on the properties of materials.

At the same time, power sources have always been a problem for wearable electronics. Traditional batteries cannot meet the increasing requirements of power supply due to their relatively rigid form factor and limited lifetime. In this case, triboelectric nanogenerators (TENGs)^{9–11} and their derivative hybridized generators^{12–19} become promising candidates to solve the problem. Hybridized electromagnetic-triboelectric nanogenerators represent one of the largest branches to enhance the output power.^{20–25} However, traditional magnets in electromagnetic generators (EMGs) are too rigid to integrate with flexible wearable devices,

and thus, there is a huge mismatch to employ them in real applications due to the high density and great hardness.

Here, we report a textile that can serve as the material for both multipurpose protective clothing and hybrid energy harvesting. We mix functional materials (i.e., CNT and NdFeB microparticles) with the PDMS matrix and adopt laser cutting to pattern the composite material into thin strips. Tuning the proportion of CNT and NdFeB microparticles yields composites with desired density, modulus, conductivity, and magnetism, suitable for wearable applications. As a protective textile, it can block 99.8% electromagnetic signals ranging from 3 MHz to 3 GHz, thus preventing people from radiations. In addition, benefiting from the features of the materials, the textile possesses good hydrophobicity flame retardancy, making it suitable for raincoat materials and fire-fighting equipment. As an energy harvester, the textile can harvest energy from human motions by contact electrification and electromagnetic induction. The maximum power density can reach 69.7 mW/m² by TENG and 8.8 W/m² by EMG. Meanwhile, the hybridized TENG and EMG textile with an area of 49 cm² can charge a 22 μF capacitor to 3 V in 110 s.

Figure 1(a) illustrates the detailed fabrication process of the composite. First, mix the solution for 20 min. After heat curing and assembling, the image of the as-fabricated textile is shown in Fig. 1(b) and magnetized by 3 T at a maximum of 35 mT by reading the gauss meter

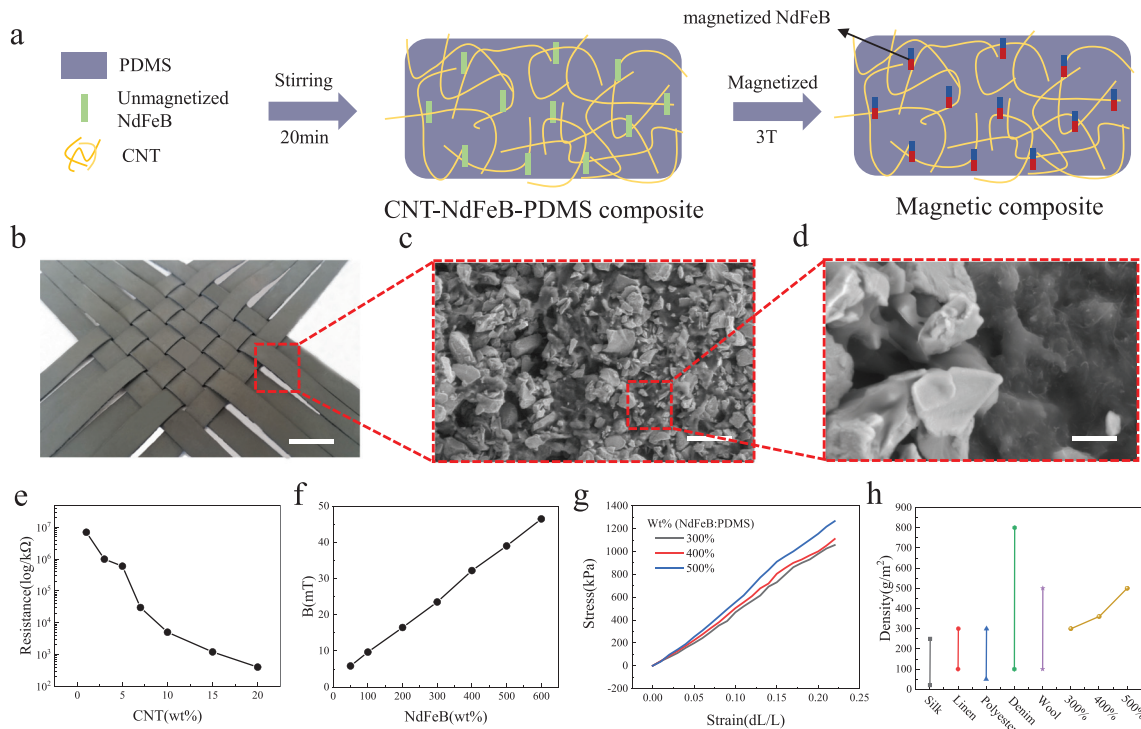


FIG. 1. (a) Fabrication of the magnetic composite. (b) Image of the textile assembled by the strip structured composite; scale bar: 1 cm. (c) SEM image of the composite; scale bar: 10 μm . (d) Locally amplified SEM image of the composite; scale bar: 1 μm . (e) Stress-strain curve of the composite with different NdFeB: PDMS weight ratios. (f) Density comparison of the textile with traditional materials. (g) Resistance at different CNT weight ratios. (h) Magnetic flux density at different NdFeB weight ratios.

finally in Fig. S1. The scanning electron microscope (SEM) images in Figs. 1(c) and 1(d) clearly show that the NdFeB microparticles and CNT spread inside the composite and help the composite become magnetic and conductive.

With respect to the composite, results in Fig. 1(e) suggest that the resistance of the composite has a negative relationship with CNT's proportion because the more the CNTs are connected, the better the conductivity composite can be obtained. At the same time, the magnetic flux density shows a reversed trend as shown in Fig. 1(f) that more NdFeB microparticles can achieve stronger magnetism after being pulse magnetized. In the meantime, NdFeB accounts for the most of the weight proportion. Therefore, to reach a modest wearability, the study of the weight ratio of NdFeB's effect on tensile property and the density of the textile is necessary. Figures 1(g) and 1(h) show that a ratio of 4 (NdFeB: PDMS) yields textiles that can mutually benefit from the tensile property and the density as a wearing material. As a result, PDMS, CNT, and NdFeB with the weight ratio of 1:0.2:4 are the most suitable choice for the textile in this work, which can also endure the bending test for over 1000 cycles in Fig. S2.

CNT brings the textile conductivity and, thus, allows the textile to block electromagnetic signals excellently so that it can protect pregnant woman from radiation damage as shown in Fig. 2(a). First, we doped PDMS only with 400% NdFeB to check if magnetism impacts the electromagnetic shielding effect. Figure 2(b) illustrates that the magnetic sample has a better shielding effect at a relatively high frequency signal. According to the formula $SE(\text{dB}) = 20\log(E_{in}/E_{out})$, the

efficiency of shielding [Fig. 2(c)] from the magnetic composite can block more than 58% electromagnetic signals ranging from 3 MHz to 3 GHz. After doping another 20% CNT to the composite, the shielding effect improves a lot [Figs. 2(d) and 2(e)]. Specifically, CNT-PDMS and CNT-NdFeB-PDMS textile can block more than 98.7% and 99.4% signals ranging from 3 MHz to 3 GHz. Adding the flexible printed circuit board (FPCB) coil to the device to form the hybridized TENG-EMG additionally increases the shielding efficiency to 99.8%, which is in line with the products in the market.

PDMS-based textile is also a possible choice for water proofing equipment like raincoat [Fig. 3(a)], due to the hydrophobic nature of PDMS. In the hydrophobic angle test in Fig. 3(b), the PDMS's hydrophobic angle is 108.2° . After doping 20% CNT, the hydrophobicity rises to 132.1° because CNT is extremely hydrophobic. A subsequent doping of 400% NdFeB reduces the hydrophobic angle to 127.3° , a level that is enough to build hydrophobic surfaces. Here, we wash the textile with running water and dry the textile naturally, it does not significantly influence the output of the TENG and EMG, as presented in Figs. 3(c) and 3(d), and the surface topography bears almost no changes as shown in Fig. S3. Figures 3(e) and 3(f) demonstrate the stable resistance, magnetic flux density, and the output of the TENG and EMG after being immersed in water for 6 days. The electromagnetic shielding efficiency remains over 99% [Fig. 3(g)], proving that the textile is a wonderful candidate for water proofing clothing.

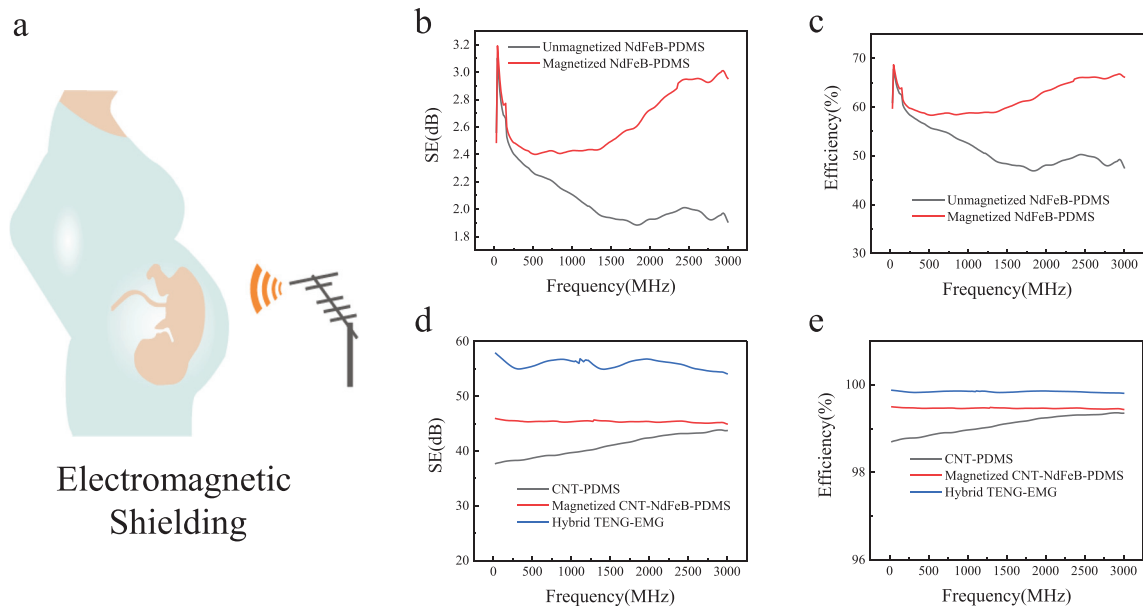


FIG. 2. Electromagnetic shielding performance of the textile. (a) Schematic illustration of electromagnetic shielding. (b) and (c) measured shielding effectiveness (SE) and efficiency of unmagnetized and magnetized NdFeB-PDMS composites. (d) and (e) measured shielding effectiveness (SE) and efficiency of the CNT PDMS, magnetized CNT-NdFeB-PDMS composite, and TENG-EMG device.

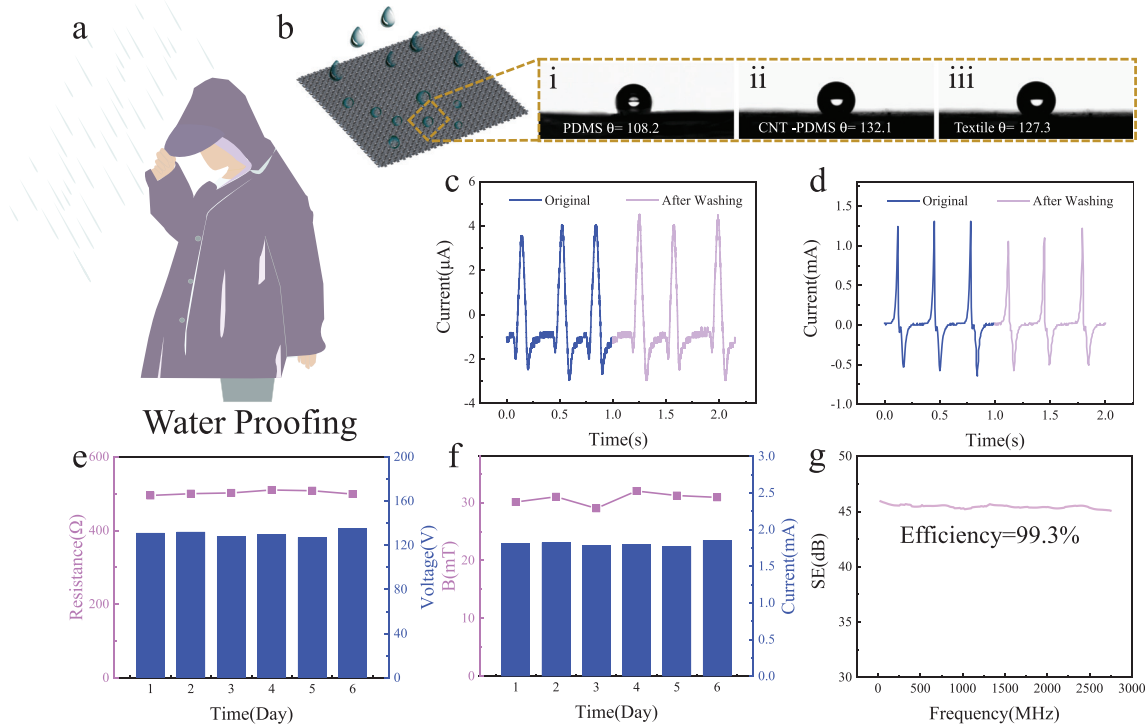


FIG. 3. Water proofing performance of the textile. (a) Schematic illustration of the water proofing function. (b) Hydrophobic angle of PDMS, CNT-PDMS, and textile. (c) and (d) TENG's and EMG's output comparison before and after the textile goes through the rain wash. (e) Resistance and TENG's output with the device immersing in water ranging from 1 to 6 days. (f) Magnetic flux density and EMG's output with the device immersing in water ranging from 1 to 6 days. (g) Measured shielding effectiveness of the textile after rain wash.

Due to the properties of the composites, the textile is flame retardant, thereby opening avenues to building fire-fighting equipment as shown in Fig. 4(a). Heating the textile on the hot plate for 400 s at 350 °C decreases the magnetic flux density gradually to 1 mT as illustrated in Fig. 4(b). Fixing the heating time at 300 s and changing the heating temperature from 20 °C to 350 °C yield a set of values of the magnetic flux density. The magnetic flux density increases with the temperature from 20 °C to 100 °C and then decreases, showing a different trend from traditional magnets [Fig. 4(c)]. Such results are possibly due to the composite network of the PDMS matrix and NdFeB microparticles. When heating, the internal PDMS network collapses and contracts, leading to a smaller distance between magnetic NdFeB microparticles, thus enhancing the magnetic flux density. However, the magnetic flux density of NdFeB has a negative relationship with the temperature. The combined effect from two influence factors yields a relationship that is not monotonous. In the same way, the overall trend is negative by the time but not a monotonous process as presented in Figs. 4(d) and 4(e) in the case of fire burning. After burning in fire, there are little changes that happen to the resistance of

the textile; however, the magnetic flux density drops from 33 mT to extremely low, but after remagnetization, it recovers to 24 mT [Fig. 4(f)] and the relative TENG's and EMG's output corresponds to the resistance and magnetic flux density changes as shown in Fig. 4(g). At the same time, the electromagnetic shielding efficiency remains as the resistance, which is 99.21%, demonstrating a great reliability [Fig. 4(h)].

The composite can serve as a flexible permanent magnet due to the embedded NdFeB microparticles. Further integration with a flexible printed circuit board (FPCB) coil [Figs. 5(a) and S4] can enable the capability of mechanical energy harvesting from human motions. The textile with 20% CNT can also function as a single electrode TENG to generate electricity with a peak to peak open-circuit voltage of 139 V and a short-circuit current of 6.1 μ A [Figs. 5(b) and 5(c)]. At the same time, through electromagnetic induction, the EMG (with 400% NdFeB) can produce a peak to peak open-circuit voltage of 3.82 V and a short-circuit current of 1.83 mA [Figs. 5(d) and 5(e)]. Both output of TENG and EMG can endure the longtime reliability test for 3000 cycles, which proves its stability as shown in Fig. S5. The output of

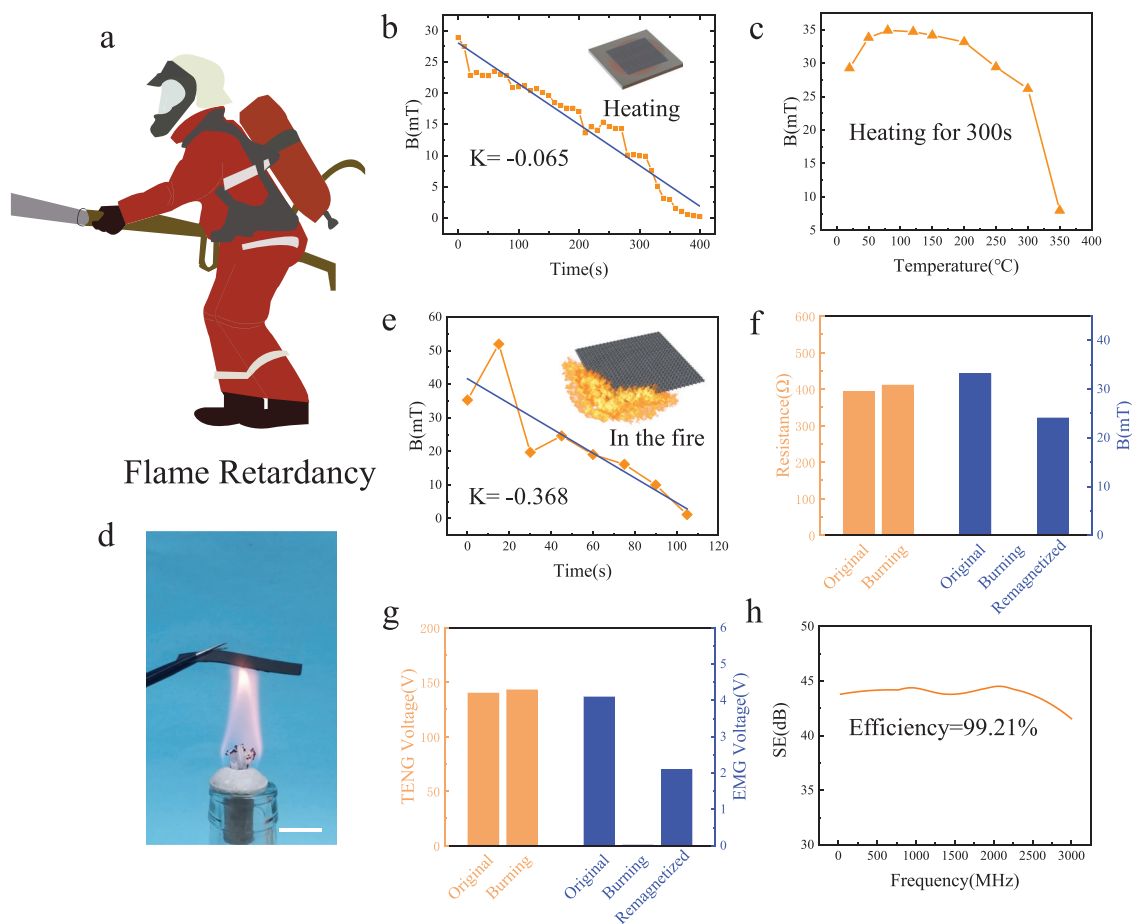


FIG. 4. Flame retardancy performance of the textile. (a) Schematic illustration of the flame retardancy scenario. (b) Magnetic flux density when heating at 350 °C. (c) Magnetic flux density when heating at different temperatures for 300 s. (d) Image of the composite heating on the fire; scale bar: 1 cm. (e) Magnetic flux density when textile is in the fire. (f) Resistance and magnetic flux density of textile in the original state, after burning and after remagnetization. (g) Measured shielding effectiveness of textile after burning.

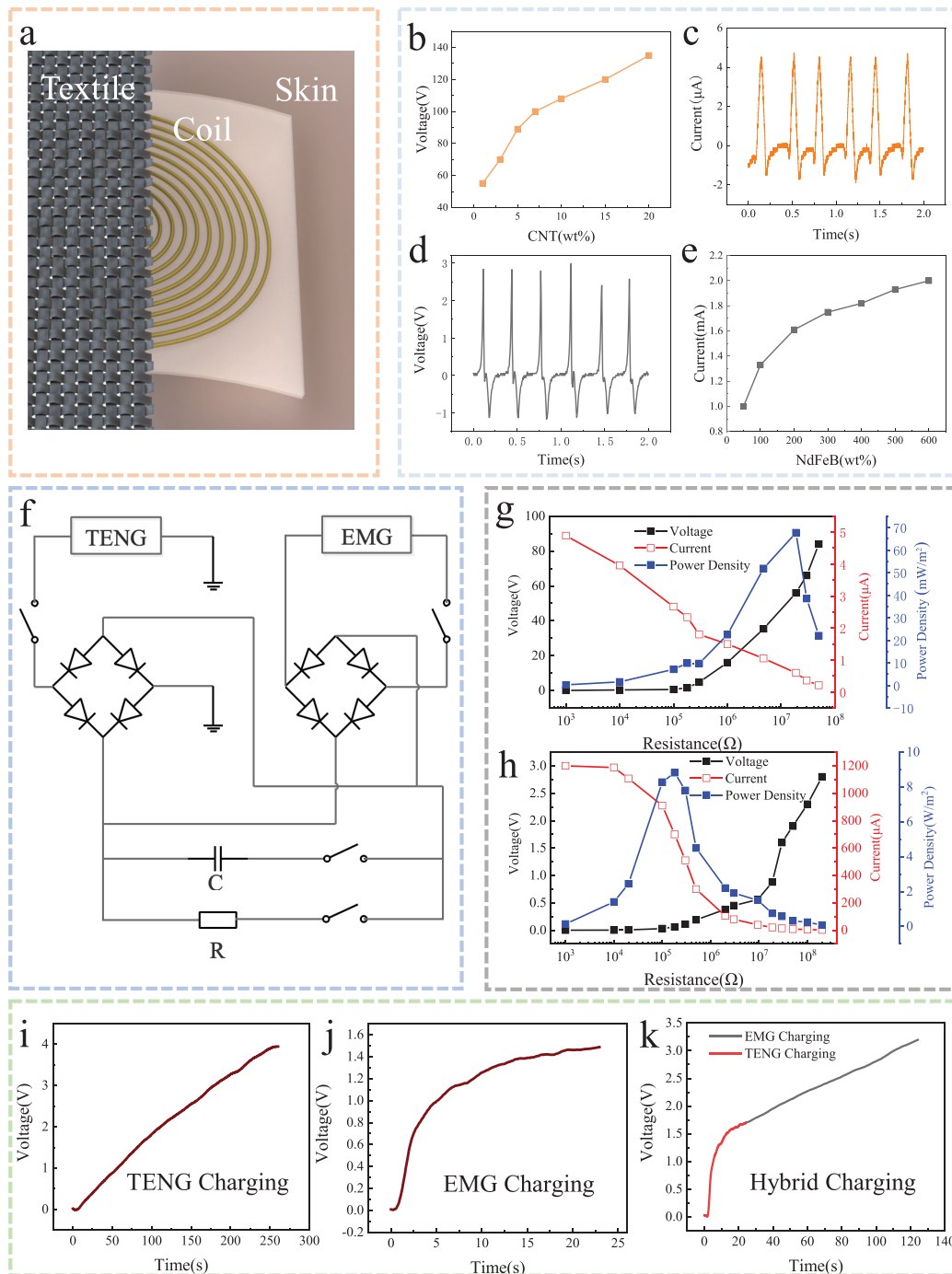


FIG. 5. Energy harvesting performance of the textile. (a) schematic illustration of the generators. (b) and (c) Voltage at different CNT percentages and currents at 20% CNT output of the TENG. (d) and (e) voltage at 400% NdFeB and current at different NdFeB percentage output of the EMG. (f) Configuration of the rectified circuits to TENG and EMG with external loads. (g) and (h) impedance matching of the TENG's and EMG's output. (i)–(k) Charging behavior of the capacitor of 22 μF by TENG only, EMG only, and hybridized generator.

TENG and EMG can be rectified to charge a capacitor [Fig. 5(f)]. The TENG has a maximum power density of 69.7 mW/m^2 when the loading resistance is $18.8 \text{ M}\Omega$ [Fig. 5(g)], and the EMG has a maximum power density of 8.8 W/m^2 at $20 \text{ K}\Omega$ [Fig. 5(h)].

TENG can charge a capacitor to a high voltage level but with slow speed [Fig. 5(i)], while EMG can charge fast but can only reach a low voltage [Fig. 5(j)]. Figure 5(k) demonstrates the hybridized charging effect that not only can charge the capacitor fast at the beginning

but also can achieve a high voltage eventually. As a result, the 22 μF capacitor can reach 3 V in 110 s, which is more efficient than charging with only TENG or EMG.

In this paper, we propose a flexible textile for multipurpose protection and hybrid energy harvesting. As material for protective clothing, the textile can block more than 99.8% electromagnetic signals, thus protecting people from radiations. Additionally, the hydrophobicity of the textile makes it possible to serve as the material for raincoat. Besides, due to the property of flame retardancy, the textile has chances to be employed in fire-fighting equipment. As an energy harvesting device, the textile possesses good energy extraction performances with a power density of more than 8.8 W/m^2 . Therefore, with the conductive and magnetic composite, the textile provides possibilities in multipurpose protective clothing and wearable energy harvesting devices.

See the [supplementary material](#) for the AFM images of the unmagnetized and magnetized composite (Fig. S1), bending test of the textile (Fig. S2), SEM image of the composites after rain wash (Fig. S3), optical image of hybridized generator (Fig. S4), and cycling reliability (Fig. S5).

This work was supported by the National Key R&D Project from Minister of Science and Technology, China (No. 2016YFA0202701), and the National Natural Science Foundation of China (Grant No. 61674004).

The authors declare no conflict of interest.

DATA AVAILABILITY

The data that support the findings of this study are available from the corresponding author upon reasonable request.

REFERENCES

1. Ding, K. H. Chan, Y. Zhou, X. Wang, Y. Cheng, T. Li, and W. Ho, "Scalable thermoelectric fibers for multifunctional textile-electronics," *Nat. Commun.* **11**, 6006 (2020).
2. J. Shi, S. Liu, L. Zhang, B. Yang, L. Shu, Y. Yang, M. Ren, Y. Wang, J. Chen, W. Chen, Y. Chai, and X. Tao, "Smart textile-integrated microelectronic systems for wearable applications," *Adv. Mater.* **32**, 1901958 (2020).
3. H. Bae, B. Jang, H. Park, S. Jung, H. Lee, J. Park, S. Jeon, G. Son, W. Tcho, K. Yu, S. Im, S. Choi, and Y. Choi, "Functional circuitry on commercial fabric via textile-compatible nanoscale film coating process for fibertronics," *Nano Lett.* **17**, 6443–6452 (2017).
4. Q. Zhang, Q. Liang, Z. Zhang, Z. Kang, Q. Liao, Y. Ding, M. Ma, F. Gao, X. Zhao, and Y. Zhang, "Electromagnetic shielding hybrid nanogenerator for health monitoring and protection," *Adv. Funct. Mater.* **28**, 1703801 (2018).
5. Z. Ma, S. Kang, J. Ma, L. Shao, Y. Zhang, C. Liu, A. Wei, X. Xiang, L. Wei, and J. Gu, "Ultraflexible and mechanically strong double-layered aramid nanofiber-Ti₃C₂Tx MXene/silver nanowire nanocomposite papers for high-performance electromagnetic interference shielding," *ACS Nano* **14**, 8368–8382 (2020).
6. M. Sang, S. Wang, S. Liu, M. Liu, L. Bai, W. Jiang, S. Xuan, and X. Gong, "A hydrophobic, self-powered, electromagnetic shielding PVDF based wearable device for human body monitoring and protection," *ACS Appl. Mater. Interfaces* **11**, 47340–47349 (2019).
7. L. Ma, R. Wu, S. Liu, A. Patil, H. Gong, J. Yi, F. Sheng, Y. Zhang, J. Wang, J. Wang, W. Guo, and Z. Wang, "A machine-fabricated 3D honeycomb-structured flame-retardant triboelectric fabric for fire escape and rescue," *Adv. Mater.* **32**, 2003897 (2020).
8. R. Cheng, K. Dong, L. Liu, C. Ning, P. Chen, X. Peng, D. Liu, and Z. Wang, "Flame-retardant textile-based triboelectric nanogenerators for fire protection applications," *ACS Nano* **14**, 15853–15863 (2020).
9. H. Zou, Y. Zhang, L. Guo, P. Wang, X. He, G. Dai, H. Zheng, C. Chen, A. Wang, C. Xu, and Z. Wang, "Quantifying the triboelectric series," *Nat. Commun.* **10**, 1427 (2019).
10. X. Zhang, M. Han, R. Wang, B. Meng, F. Zhu, X. Sun, W. Hu, W. Wang, Z. Li, and H. Zhang, "High-performance triboelectric nanogenerator with enhanced energy density based on single-step fluorocarbon plasma treatment," *Nano Energy* **4**, 123–131 (2014).
11. W. Tang, Y. Han, C. Han, C. Gao, X. Cao, and Z. Wang, "Self-powered water splitting using flowing kinetic energy," *Adv. Mater.* **27**, 272–276 (2015).
12. M. Han, X. Zhang, B. Meng, W. Liu, W. Tang, X. Sun, W. Wang, and H. Zhang, "r-Shaped hybrid nanogenerator with enhanced piezoelectricity," *ACS Nano* **7**, 8554–8560 (2013).
13. M. Zhu, Q. Shi, T. He, Z. Yi, Y. Ma, B. Yang, T. Chen, and C. Lee, "Self-powered and self-functional cotton sock using piezoelectric and triboelectric hybrid mechanism for healthcare and sports monitoring," *ACS Nano* **13**, 1940–1952 (2019).
14. X. Chen, Z. Ren, M. Han, J. Wan, and H. Zhang, "Hybrid energy cells based on triboelectric nanogenerator: From principle to system," *Nano Energy* **75**, 104980 (2020).
15. Y. Chen, Y. Cheng, Y. Jie, X. Cao, N. Wang, and Z. Wang, "Energy harvesting and wireless power transmission by a hybridized electromagnetic-triboelectric nanogenerator," *Energy Environ. Sci.* **12**, 2678–2684 (2019).
16. Y. Wu, X. Wang, Y. Yang, and Z. Wang, "Hybrid energy cell for harvesting mechanical energy from one motion using two approaches," *Nano Energy* **11**, 162–170 (2015).
17. X. Wang and Y. Yang, "Effective energy storage from a hybridized electromagnetic-triboelectric nanogenerator," *Nano Energy* **32**, 36–41 (2017).
18. K. Zhang, Z. Wang, and Y. Yang, "Conductive fabric-based stretchable hybridized nanogenerator for scavenging biomechanical energy," *ACS Nano* **10**, 4728–4734 (2016).
19. T. Quan, Y. Wu, and Y. Yang, "Hybrid electromagnetic-triboelectric nanogenerator for harvesting vibration energy," *Nano Res.* **8**, 3272–3280 (2015).
20. T. Quan and Y. Yang, "Fully enclosed hybrid electromagnetic-triboelectric nanogenerator to scavenge vibrational energy," *Nano Res.* **9**, 2226–2233 (2016).
21. T. Quan, Z. Wang, and Y. Yang, "A shared-electrode-based hybridized electromagnetic-triboelectric nanogenerator," *ACS Appl. Mater. Interfaces* **8**, 19573–19578 (2016).
22. K. Zhang and Y. Yang, "Linear-grating hybridized electromagnetic-triboelectric nanogenerator for sustainably powering portable electronics," *Nano Res.* **9**, 974–984 (2016).
23. X. Chen, H. Guo, H. Wu, H. Chen, Y. Song, Z. Su, and H. Zhang, "Hybrid generator based on freestanding magnet as all-direction in-plane energy harvester and vibration sensor," *Nano Energy* **49**, 51–58 (2018).
24. J. Wan, H. Wang, L. Miao, X. Chen, Y. Song, H. Guo, C. Xu, Z. Ren, and H. Zhang, "A flexible hybridized electromagnetic-triboelectric nanogenerator and its application for 3D trajectory sensing," *Nano Energy* **74**, 104878 (2020).
25. L. Gao, S. Lu, W. Xie, X. Chen, L. Wu, T. Wang, A. Wang, C. Yue, D. Tong, W. Lei, H. Yu, X. He, X. Mu, Z. Wang, and Y. Yang, "A self-powered and self-functional tracking system based on triboelectric-electromagnetic hybridized blue energy harvesting module," *Nano Energy* **72**, 104684 (2020).